Unsupervised Image Segmentation for Passive THz Broadband Images for Concealed Weapon Detection *

Mabel D. Ramírez †, Charles R. Dietlein†‡, Erich Grossman‡, Zoya Popović†

†Department of Electrical and Computer Engineering
Campus Box 425, University of Colorado at Boulder, Boulder, CO, 80309-0425

‡National Institute of Standards and Technology
325 Broadway, Boulder, CO, 80305

ABSTRACT

This work presents the application of a basic unsupervised classification algorithm for the segmentation of indoor passive Terahertz images. The 30,000 pixel broadband images of a person with concealed weapons under clothing are taken at a range of 0.8-2 m over a frequency range of 0.1-1.2 THz using single-pixel row-based raster scanning. The spiral-antenna coupled 36x1x0.02 μm Nb bridge cryogenic micro-bolometers are developed at NIST-Optoelectronics Division. The antenna is evaporated on a 250 μm thick Si substrate with a 4 mm diameter hyper-hemispherical Si lens. The NETD of the microbolometer is 125 mK at an integration time of 30 ms. The background temperature calibration is performed with a known 25 pixel source above 330 K, and a measured background fluctuation of 200-500 mK. Several weapons were concealed under different fabrics: cotton, polyester, windblocker jacket and thermal sweater. Measured temperature contrasts ranged from 0.5-1 K for wrinkles in clothing to 5 K for a zipper and 8 K for the concealed weapon. In order to automate feature detection in the images, some image processing and pattern recognition techniques have been applied and the results are presented here. We show that even simple algorithms, that can potentially be performed in real time, are capable of differentiating between a metal and a dielectric object concealed under clothing. Additionally, we show that pre-processing can reveal low temperature contrast features, such as folds in clothing.

Keywords: T erahertz, broadband images, clustering, segmentation, image processing, concealed weapon detection

1. INTRODUCTION

Growing interest in the millimeter wave region of the electromagnetic spectrum has prompted numerous scientific and application studies in civil and military fields. Many atoms and molecules contain transitions in the Terahertz frequency range. Electromagnetic waves at this frequency range can penetrate common clothing materials making them appropriate for applications in concealed weapon detection (CWD). Classical image processing, pattern recognition, and target detection techniques can be applied to automate the process of concealed weapon detection. The challenges for image processing are a result of poor signal-to-noise ratio (SNR), broadband integration, and low number of pixels as compared to standard optical images. The 30,000 pixel broadband images of a person with concealed objects under clothing are taken at a range of 0.8-2 m over a frequency range of 0.1-1.2 THz using single-pixel row-based raster scanning. The spiral-antenna coupled 36x1x0.02 μm Nb bridge cryogenic micro-bolometers are developed at NIST-Optoelectronics Division. The antenna is evaporated on a 250 μm thick Si substrate with a 4 mm diameter hyper-hemispherical Si lens. The noise equivalent temperature difference (NETD) of the microbolometer is 125 mK at an integration time of 30 ms. The background temperature calibration is performed with a known hot-spot at 330 K, and the measured background fluctuation was 200-500 mK. Further details of the imaging system have been presented previously. [1,2,3,4]

Prior to segmentation, the measured relative power data is calibrated and transformed into a radiometric temperature image in Kelvin. The algorithm presented here is described in Fig.1. The image is pre-processed using an adaptive spatial noise removal filter prior to segmentation. This filter eliminates white Gaussian noise that is present in the scene and is

*NIST is a US Government organization, therefore this work is not subject to copyright.

M.D.R.: E-mail: ramirezv@colorado.edu
Telephone: 1 303 492 8998

Terahertz for Military and Security Applications V, edited by James O. Jensen, Hong-Liang Cui,
Proc. of SPIE Vol. 6549, 65490J, (2007) · 0277-786X/07/$18 · doi: 10.1117/12.720004

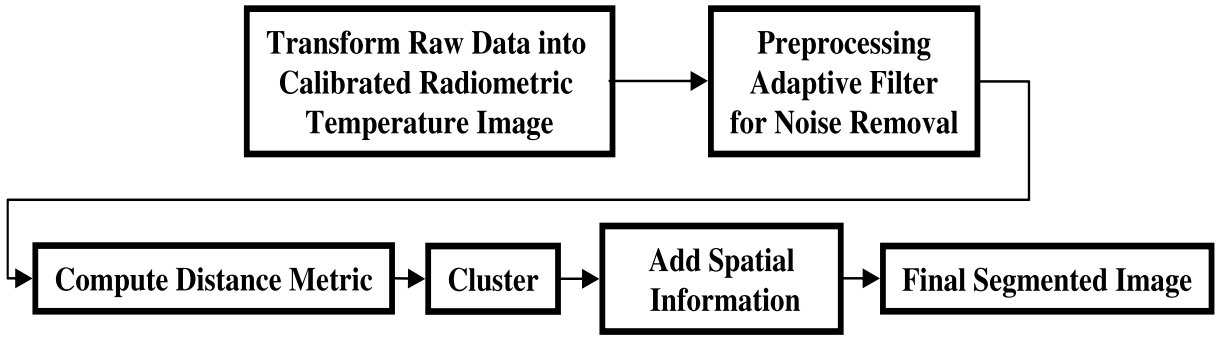


Figure 1. Algorithm for the segmentation of indoor passive Terahertz images for concealed weapon detection

caused by instrumentation. After filtering the image, a distance metric is computed on a pixel by pixel basis. The image is then divided into eight different clusters. Each of the pixels are grouped based on the information obtained by the Euclidean and Mahalanobis distance calculation. The number of clusters is selected as a compromise between minimizing the centroid error within each cluster while maintaining a reasonable pixel count per cluster. Some prior knowledge of the scene is used for determining the number of clusters, e.g. knowing that the isothermal human body should be one cluster. Spatial information is added to the algorithm expecting that spatially neighboring pixels will not contain drastic temperature changes. The addition of spatial information to an unsupervised classification algorithm has been previously used for hyperspectral image classification.[5,6]

The paper is organized as follows. Section 2 gives a description of the algorithm while Section 3 presents the raw and processed images. A discussion of the results including suggestion for different pre-processing are given in Section 4.

2. SEGMENTATION ALGORITHM

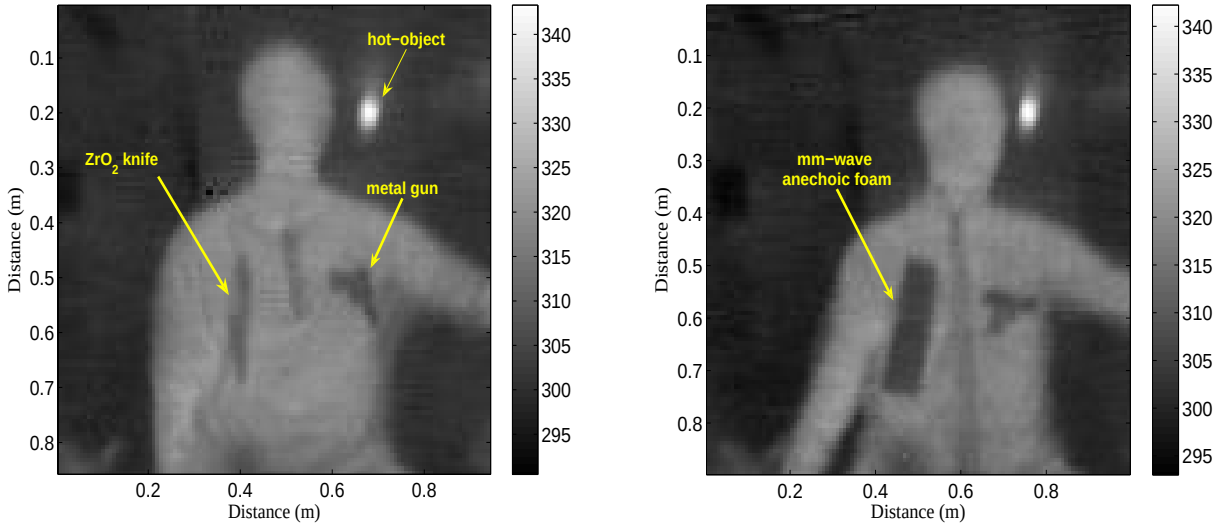
Unsupervised pattern recognition techniques offer the advantage of automatic clustering of any given dataset without the need of *a priori* class information. In unsupervised mechanisms, the clustering is performed by computing a similarity measure across the pixels in the image by a given distance metric. A commonly used techniques is the k-means clustering. This algorithm groups statistically similar data points by the information obtained from the Euclidean distance and the estimated mean for each of the classes. The Euclidean distance measures the similarity between pixel values $\boldsymbol{x_i}$ and $\boldsymbol{x_j}$ as

$$d_E^2(\boldsymbol{x_i}, \boldsymbol{x_j}) = (\boldsymbol{x_i} - \boldsymbol{x_j})^T(\boldsymbol{x_i} - \boldsymbol{x_j}) = |x_i - x_j|^2 \tag{1}$$

In this case, the pixels are one dimensional: $\boldsymbol{x_i}$ and $\boldsymbol{x_j}$ are single valued and are measured in degrees Kelvin. Therefore, points in the image containing similar radiometric temperatures will be considered *close* to each other, although they can be spatially separated. The iterative procedure of the traditional k-means algorithm with Euclidean distances will not be discussed in this paper and can be found in a number of references.[7,8] In this work, we use the Mahalanobis distance as the metric. This metric is similar to the Euclidean distance, however it also takes into consideration the variability of the sample points. The Mahalanobis distance is given by

$$d_M^2(\boldsymbol{x_i}, \boldsymbol{x_j}) = (\boldsymbol{x_i} - \boldsymbol{x_j})^T\Sigma^{-1}(\boldsymbol{x_i} - \boldsymbol{x_j}) = \frac{|x_i - x_j|^2}{\sigma} \tag{2}$$

where Σ is the covariance matrix defined as the expected value of $E[(\boldsymbol{x_i} - \mu_i)(\boldsymbol{x_j} - \mu_j)^T]$ and can be reduced to the standard deviation, σ, for single valued pixels. It can be observed that Eqn. (1) is the special case of Eqn. (2) when $\Sigma = I$.



(a) Concealed ZrO_2 knife and metal gun

(b) Concealed millimeter wave anechoic foam and metal gun

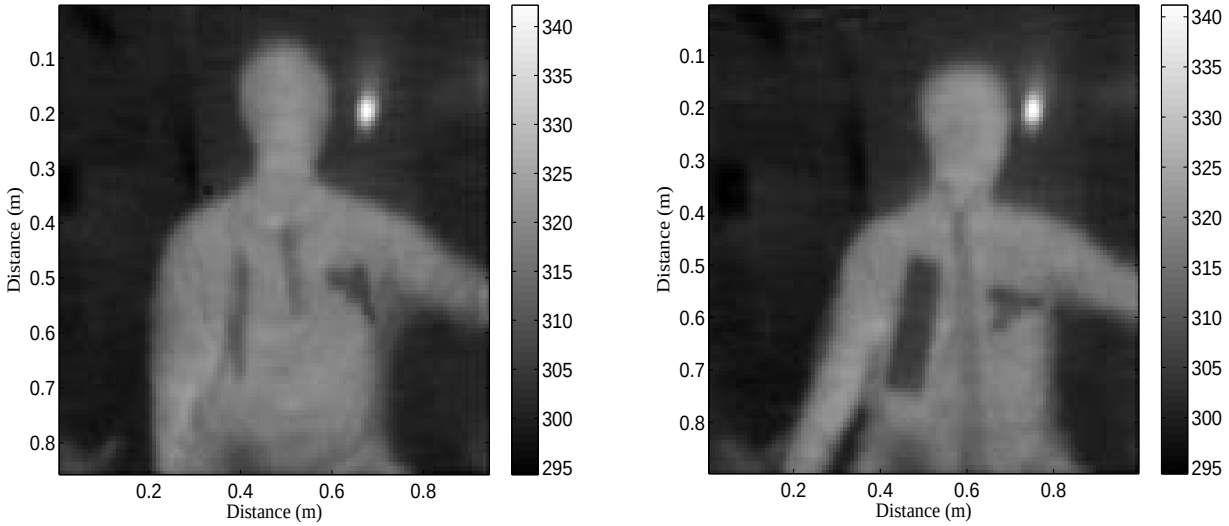
Figure 2. Calibrated Images. Gray scale represents radiometric temperature in degrees Kelvin. A 25 pixel hot-object is used for calibration above 330 K

The segmentation algorithm images is divided in two stages: (1) segment the temperature image data with a clustering algorithm; and (2) post-processing: addition of spatial information using k-nearest neighbors (k-NN). The k-NN algorithm [7] computes the spatial distance from a sample point to another. An unknown sample is classified to a nearest or similar sample point from the set. In this paper, the k-NN is used as the second stage of the algorithm. Sample points contained in the 2x2 nearest neighborhood is used to determine the final segmentation.

3. MEASURED AND PROCESSED IMAGE

The 30,000 pixel broadband images of a person with concealed weapons under clothing are taken at a range of 0.8-2 m over a frequency range of 0.1-1.2 THz using single-pixel row-based raster scanning. The images shown in Fig. 2 present two examples of calibrated images prior to processing. The brightest region in the image represents the known hot object used for calibration. The knowledge of the highest (hot object) and lowest temperature (room) in the image are used to fit the pixel values from the raw relative power data to a radiometric temperature image. Several weapons ZrO_2 knife, metal gun, mm-wave anechoic foam) were concealed under different fabrics: cotton, polyester, windblocker jacket and thermal sweater. Measured temperature contrasts ranged from 0.5-1 K for wrinkles in clothing to 5 K for a zipper and 8K for the concealed weapon. Figure 3 shows the calibrated images after noise removal with a Wiener filter. The SNR increases from 19 dB for the measured relative power raw data shown in Fig. 2 to 24 dB after filtering the image in Fig. 3.

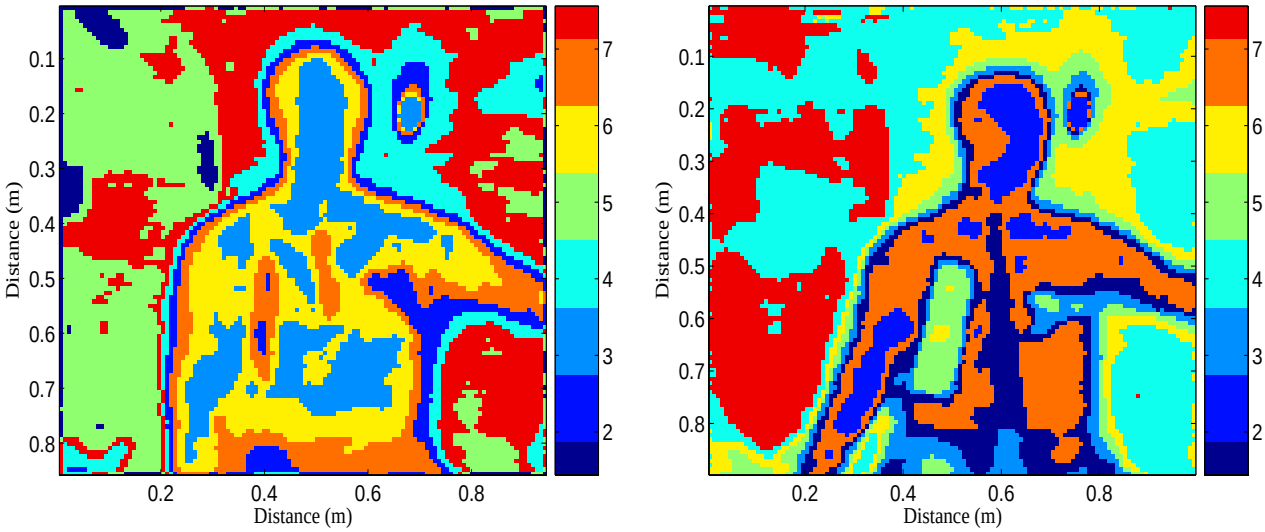
After filtering the noise, the data is subjected to the clustering algorithm. The degree of similarity among pixels is computed by the Mahalanobis distance for all pairs of pixels. After the image is divided into the desired number of clusters, a second stage of adding spatial information is applied. Nearest neighbor information is included and a final map with cluster labels is produced. For the purposes of comparison, Fig. 4 shows the segmentation results using only traditional k-means with Euclidean distance and without addition of spatial pixel neighborhood information. In the following set of figures, each of the images are displayed by cluster label. The colors from the scale represent a cluster number, each pixel of the same color is assigned to the same group. This means, for example, that if a pixel is assigned to cluster 2 in Fig. 4(a) with the ZrO_2 knife, then all *similar* pixels based on the Euclidean distance measure are assigned to cluster 2. Note that the human body has been segmented into three different clusters and that the ZrO_2 knife cannot be identified easily by observing the segmented image by k-means only. However, note that in the Mahalanobis clustered image in Fig. 5 more regions on the human subject are assigned to the same cluster. It can also be observed that the shape of the ZrO_2 knife is better reconstructed and can be visually identified by the user. Another important note is that the gun has been



(a) Concealed ZrO_2 knife and metal gun

(b) Concealed millimeter wave anechoic foam and metal gun

Figure 3. Removal of instrumentation noise by means of an adaptive two dimensional Wiener filter. The gray scale represents radiometric temperature in Kelvin



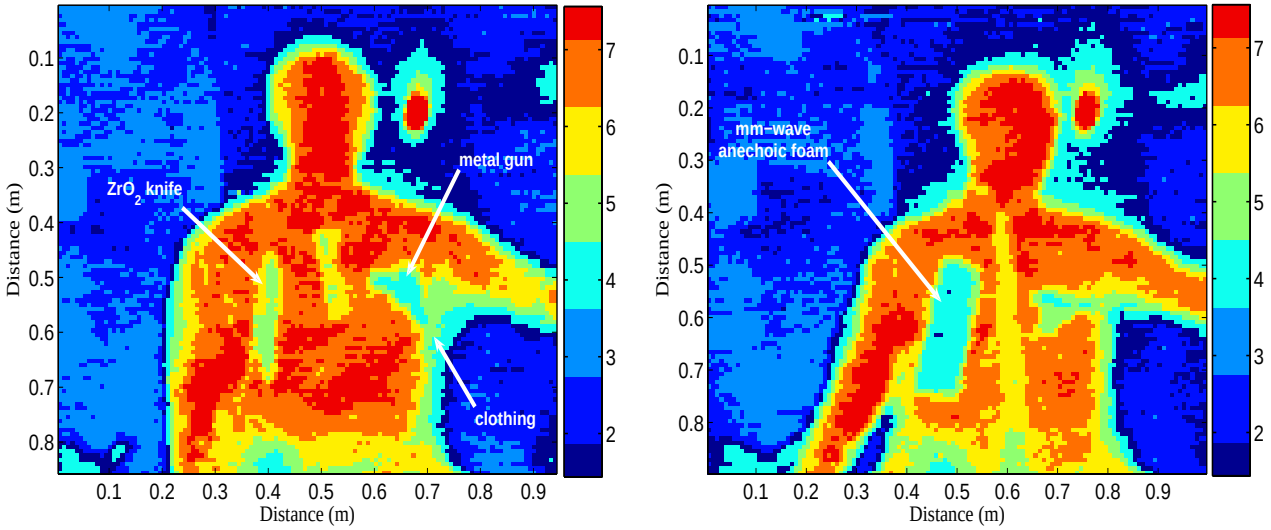
(a)

(b)

Figure 4. Application of k-means segmentation algorithm: (a) ZrO_2 knife and gun, (b) millimeter wave anechoic foam and gun. Each color represents a cluster. The segmentation is based on the Euclidean Distance criteria.

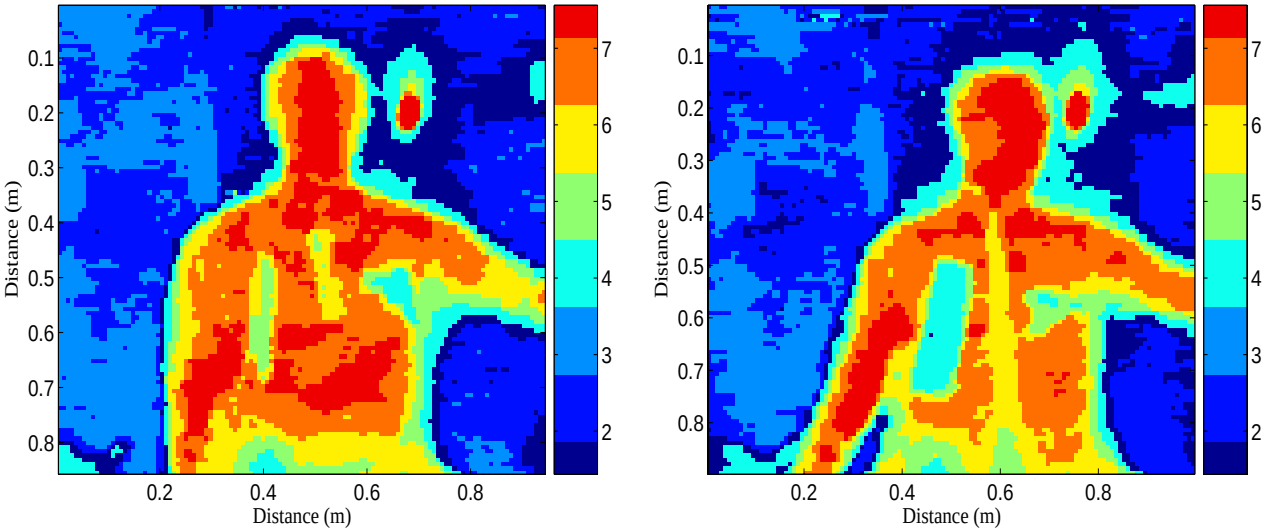
identified in Fig. 5 as pertaining to a different cluster than the human subject and the edge of the body. This discrimination cannot be observed in the images clustered by k-means only. This implies that the addition of variance information from the Mahalanobis distance computation provides the algorithm with more discriminating capabilities when compared to the results of Euclidean distance alone.

For the addition of spatial information, the 2×2 neighborhoods are calculated and samples that are spatially close are assigned the same cluster number after comparing with the segmentation results using only the Mahalanobis distance.



(a) (b)

Figure 5. Application of Mahalanobis Clustering Algorithm. Each color represents a cluster. The segmentation is based on the Mahalanobis Distance criteria.



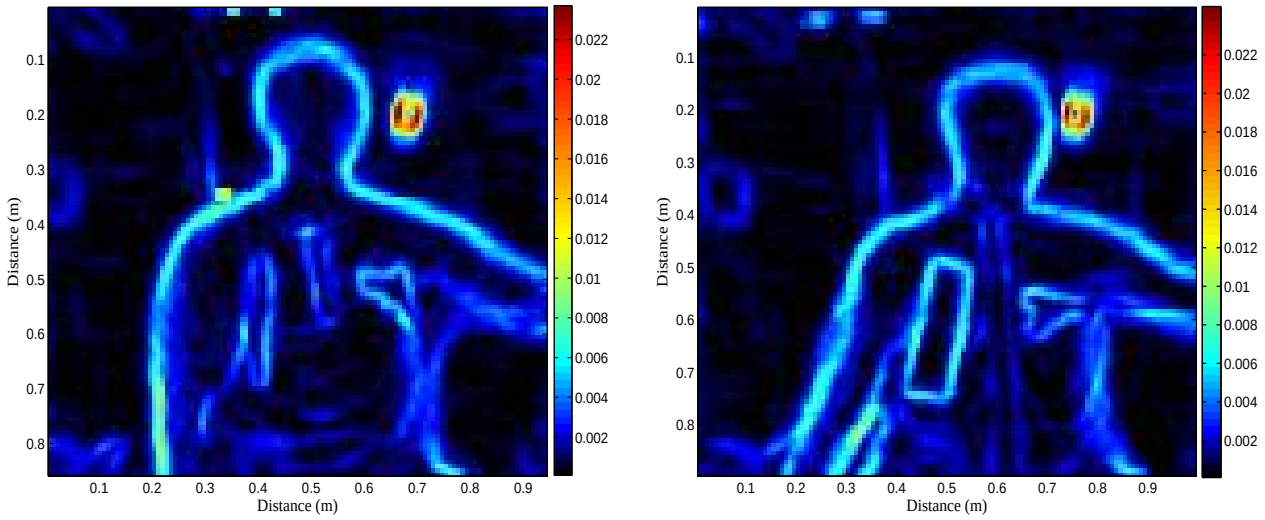
(a) (b)

Figure 6. Addition of spatial information using 4-nearest neighbors to segmented image results

The pixels are re-clustered with the information provided by the 4-NN spatial information. The resulting images with the effects of adding spatially nearest neighborhood information is shown in Fig. 6. The additional improvement in these images when using spatial information is minimal and probably not worth the extra computational time.

4. DISCUSSION

In summary, this work presents the results of segmenting passive Terahertz broadband images by using unsupervised classification mechanisms. The results of the clustering algorithms based on the computation of the Mahalanobis distance



(a) (b)

Figure 7. Pre-processing of radiometrically calibrated image using a texture analysis filter. The 3x3 spatial neighborhood standard deviation is used to reveal small temperature differences across the image allowing them to become visually obvious.

were compared to traditional techniques such as k-means clustering using only Euclidean distance. Once the images were clustered, spatial information was added to the results. The segmented images show that the concealed weapons were visually identifiable for the images clustered by the Mahalanobis distance method. In figures 2 through 6, the images were pre-processed by simple noise filtering. The noise filtering was accomplished by using a two dimensional Wiener filter that was able to remove white Gaussian noise from the data caused by instrumentation. The signal-to-noise ratio increased from 19 dB for the measured relative power raw data to 24 dB after filtering the data.

Different types of pre-processing techniques can be used to reveal other features contained in the measured images but not visible in figures 2 through 6. For example, a texture filter[9] based on the analysis of spatial standard deviation can be used. Figure 7 shows the result of processing the image with a 3×3 neighborhood standard deviation filter. The standard deviation of each 3×3 neighborhood was calculated and a new image was generated containing the resulting value for σ at each neighborhood. The use of this filter allows very small temperature differences across the image to become visually obvious. In conclusion, we show that very simple image processing techniques are useful for fast visual concealed weapon detection for the case of broadband passive millimeter wave images with low signal-to-noise ratio and low pixel count.

ACKNOWLEDGMENTS

M.D. Ramírez was supported by the NSF AGEP grant, cooperative agreement #HRD-0086551. The authors acknowledge funding under a NSF Interdisciplinary Award, #0501578. This work was supported in part by the Office of Law Enforcement Standards and the Department of Homeland Security Directorate for Science and Technology.

REFERENCES

1. A. R. Luukanen and V.-P. Viitanen, "Terahertz imaging system based on antenna-coupled microbolometers," in *Proc. SPIE Vol. 3378, p. 34-44, Passive Millimeter-Wave Imaging Technology II, Roger M. Smith; Ed.*, R. M. Smith, ed., pp. 34–44, Aug. 1998.
2. A. Luukanen and J. P. Pekola, "A superconducting antenna-coupled hot-spot microbolometer," *Applied Physics Letters* **82**, pp. 3970–3972, June 2003.

3. E. N. Grossman, A. K. Bhupathiraju, A. J. Miller, and C. D. Reintsema, "Concealed weapons detection using an uncooled millimeter-wave microbolometer system," in *Proc. SPIE Vol. 4719, p. 364-369, Infrared and Passive Millimeter-wave Imaging Systems: Design, Analysis, Modeling, and Testing, Roger Appleby; Gerald C. Holst; David A. Wikner; Eds.*, R. Appleby, G. C. Holst, and D. A. Wikner, eds., pp. 364–369, July 2002.
4. A. Luukanen, E. Grossman, A. Miller, P. Helisto, J. Pentilla, H. Sipola, and H. Seppa, "An ultra-low noise superconducting antenna-coupled microbolometer with a room-temperature readout," *Microwave and Wireless Components Letters* **16**, pp. 464– 466, August 2006.
5. L. Jimenez, J. Rivera-Medina, E. Rodriguez-Diaz, E. Arzuaga-Cruz, and M. Ramirez-Velez, "Integration of spatial and spectral information by means of unsupervised extraction and classification for homogenous objects applied to multispectral and hyperspectral data," *IEEE Transactions on Geoscience and Remote Sensing* **43**, pp. 844– 851, April 2005.
6. L. O. Jimenez-Rodriguez and J. Rivera-Medina, "Integration of spatial and spectral information in unsupervised classification for multispectral and hyperspectral data," *Proc. SPIE, Image and Signal Processing for Remote Sensing V* **3871**, pp. 24–33, December 1999.
7. R. Duda, P. Hart, and D. Stork, *Pattern Classification*, Wiley and Sons, second ed., 2000.
8. T. Hastie, R. Tibshirani, and J. Friedman, *The Elements of Statistical Learning*, Springer, 2001.
9. R. Gonzalez and R. Woods, *Digital Image Processing*, Prentice-Hall, second ed., 2002.
10. T. Yamasaki and D. Gingras, "Image classification using spectral and spatial information based on MRF models," *IEEE Trans. on Image Processing* **4**, pp. 1333–1339, September 1995.